"En face" OCT Imaging of the IS/OS Junction Line in Type 2 Idiopathic Macular Telangiectasia

Ferenc B. Sallo,[1–3] *Tunde Peto,*[4] *Catherine Egan,*[1] *Ute E. K. Wolf-Schnurrbusch,*[3] *Traci E. Clemons,*[5] *Mark C. Gillies,*[6] *Daniel Pauleikhoff,*[7] *Gary S. Rubin,*[2] *Emily Y. Chew,*[8] *Alan C. Bird,*[9] *and the MacTel Study Group*[10]

Purpose. We investigated abnormalities of the photoreceptor inner/outer segment (IS/OS) junction layer viewed "en face" and their functional correlates in type 2 idiopathic macular telangiectasia (type 2 MacTel).

Methods. Segmentation and "en face" imaging of the IS/OS lines in spectral domain optical coherence tomographic (SD-OCT) volumes were performed manually. Mesopic retinal sensitivity thresholds were determined using a Nidek MP1 microperimeter. "En face" SD-OCT images and microperimetric data were superimposed over images of the fundus. Retinal structure and characteristics of type 2 MacTel were analyzed, and associations of structural changes with function were investigated.

Results. We examined 49 eyes of 28 patients (mean age 62.6 ± 9.4 years). Total IS/OS break area ranged from 0.04 to 2.23 mm^2 (mean 0.63 mm^2, SD 0.53 mm^2) and 0.03 to 1.49 mm^2 (mean 0.49 mm^2, SD 0.42 mm^2) in right and left eyes, respectively. A correlation between fellow eyes was present (Spearman correlation $\rho = 0.770$, $P < 0.01$). An assessment of the repeatability of IS/OS lesion area measurements ($n = 19$ eyes) revealed an intra-class correlation coefficient of 0.99 (95% confidence interval [CI] of 0.975–0.996). Retinal areas corresponding to an IS/OS break showed a mean retinal sensitivity of 8.3 ± 5.8 and 8.7 ± 5.7 decibels (dB) in right and left eyes, respectively. Mean sensitivity over retinal areas outside the lesion was significantly higher, 17.0 ± 3.3 and 16.7 ± 3.6 dB in right and left eyes, respectively (paired *t*-test, $P < 0.01$). Mean aggregate retinal sensitivity loss was 33.5 ± 30.4 dB ($n = 40$), correlating well with IS/OS lesion area (Pearson correlation coefficient = 0.848, $P < 0.01$).

Conclusions. "En face" OCT imaging of the IS/OS junction layer provides a functionally relevant method for assessing disease severity in type 2 MacTel. (*Invest Ophthalmol Vis Sci.* 2012; 53:6145–6152) DOI:10.1167/iovs.12-10580

Type 2 idiopathic macular telangiectasia (type 2 MacTel) is a bilateral retinal disorder affecting the juxtafoveal region.[1] Early clinical signs may be subtle, and include a loss of retinal transparency, retinal crystals, a depletion of luteal pigment, and leakage in the fluorescein angiogram, but without retinal thickening. A disruption or cavitation of the outer retinal layers, progressive vascular remodeling, and fibrosis accompanied by pigment plaques, and retinal neovascularization scarring and atrophy limit the prognosis for central vision. The etiology and pathogenesis of the disease are understood poorly. No treatment has been proven effective in reducing the risk of central vision loss.

Optical coherence tomographic (OCT) signs of type 2 MacTel include hyporeflective spaces in the inner and outer retina, and a discontinuity (break) in the line commonly attributed to the junctions of the photoreceptor inner and outer segments (IS/OS line).[2–5]

The correlation of IS/OS abnormalities with retinal function loss and, thus, the value of the IS/OS line as a sign of photoreceptor integrity and a predictor of visual acuity has been demonstrated in vascular, metabolic, hereditary, and idiopathic retinal diseases as well as in animal models.[6–16] In type 2 MacTel, using a prototype spectral domain OCT (SD-OCT) system, Paunescu et al. found a correlation between visual acuity and the integrity of the photoreceptor layer,[17] Maruko et al. reported focal retinal function loss associated with the defects of the IS/OS line,[4] and Charbel-Issa et al. reported in a cross-sectional study of 33 type 2 MacTel patients function loss associated with outer retinal abnormalities, including an IS/OS break.[18]

Imaging the retina "en face" may facilitate assessing the topographic location of lesions and quantifying their lateral extent, as well as correlating/comparing OCT image data with other imaging modalities and functional data. Experimental OCT systems capable of producing "en face" images of the retina have been described recently.[19–25] 3D post-processing of image volumes from commercially available SD-OCT systems[26,27] may offer a flexible alternative for extracting the information of interest from readily available data without the necessity for dedicated hardware.

Our aim was to investigate the morphology of the IS/OS layer viewed "en face" and its functional relevance in type 2

From the Departments of [1]Research and Development and [9]Inherited Eye Disease, Moorfields Eye Hospital, London, United Kingdom; [2]UCL Institute of Ophthalmology, London, United Kingdom; [3]Bern Photographic Reading Centre, Department of Ophthalmology, Bern University Hospital, Bern, Switzerland; [4]NIHR Biomedical Research Centre for Ophthalmology at Moorfields Eye Hospital NHS Foundation Trust and UCL Institute of Ophthalmology, London, United Kingdom; [5]The EMMES Corporation, Rockville, Maryland; [6]Save Sight Institute, University of Sydney, Sydney, Australia; [7]St. Franziskus Hospital, Münster, Germany; and [8]National Eye Institute, National Institutes of Health, Bethesda, Maryland.

[10]See the Appendix for the members of the MacTel Study Group.

Supported by the Lowy Medical Research Institute (LMRI) and the NIHR.

Submitted for publication July 12, 2012; revised August 9, 2012; accepted August 12, 2012.

Disclosure: **F.B. Sallo**, None; **T. Peto**, None; **C. Egan**, None; **U.E.K. Wolf-Schnurrbusch**, None; **T.E Clemons**, None; **M.C. Gillies**, None; **D. Pauleikhoff**, None; **G.S. Rubin**, None; **E.Y. Chew**, None; **A.C. Bird**, None

Corresponding author: Ferenc B. Sallo, The Reading Centre, Department of Research and Development, Moorfields Eye Hospital NHS Foundation Trust, 162 City Road, London, EC1V 2PD, UK; Ferenc.Sallo@moorfields.nhs.uk.

MacTel by imaging optical density data from a commercially available SD-OCT system along a surface defined by the IS/OS lines within a volume scan.

Methods

Patients

Participants with type 2 MacTel and discontinuity of the IS/OS junction line apparent in SD-OCT B-scans were selected from the cohort of the MacTel project, an international multicenter prospective study of the natural history of type 2 MacTel, currently involving 27 research centers worldwide. Eyes with subretinal neovascularization or dense superficial pigment plaques obscuring the deeper layers of the retina were excluded. The study protocol adhered to the tenets of the Declaration of Helsinki and was approved by the institutional ethics committee of each participating center. Written, informed consent was obtained from each participant after explanation of the nature of the study.

Imaging

Standard 30° stereo field 2 color (CF) and red-free (RF) images of the fundus were recorded digitally. Standard OCT volume scans consisting of 128 B-scans within a 6×6 mm retinal area, with a resolution of 512 A-scans per B-scan were acquired using a Topcon 3D-OCT1000 unit (Topcon Medical Systems, Inc., Oakland, NJ). To assess repeatability, two consecutive OCT volume scans were collected of 20 eyes, with a few minutes' interval.

Image Processing

Correction of image registration within the volume and segmentation of the IS/OS line were performed manually, using dedicated 3D image analysis software (Visage Imaging Amira v5.3.3; Pro Medicus Ltd., Richmond, Victoria, Australia). "En face" images with a thickness of one pixel defined by the segmentation lines were exported in grayscale using orthogonal projection.

"En face" images were resampled in Adobe Photoshop CS5 Extended (Adobe Systems, Inc., San Jose, CA), and a 3×3 pixel normal (Gaussian) filter was applied to reduce high-frequency noise and the horizontal striping emanating from slight misalignments and variation in reflectivity between individual B-scans within the OCT volume. Edge detection and delineation of the IS/OS lesions were performed manually with the aid of thresholding. Wherever necessary, "en face" OCT images were analyzed in parallel with corresponding individual B-scans to identify and determine the extent of retinal structures within the area of the IS/OS break in the "en face" image. IS/OS break area and the radial distance of the nearest lesion edge from the anatomic center of the fovea were measured, expressed in pixels. An approximate calibration of distances within the "en face" image to metric units was performed based on the uniform 6 mm width of the scan raster. We acknowledge that correct calibration of measurements within OCT images requires consideration of the axial length and the refractive power of the eye. In our study these data were not collected, and "typical" values were used as provided by the manufacturer. Second area measurements for assessment of repeatability were performed by one grader after an interval of at least three weeks.

Functional Testing

Monocular best-corrected visual acuities (BCVA) were determined according to a standardized protocol, using the Early Treatment Diabetic Retinopathy Study LogMAR visual acuity charts at a distance of 4 m. Scoring of the test was based on the number of letters read correctly. Possible scores ranged from 0 (Snellen equivalent <20/800) to 100 (Snellen equivalent 20/12).[28,29]

Automated fundus-correlated microperimetry was performed using a Nidek MP1 microperimeter (Navis software version 1.7.3; MP1 Nidek Technologies, Albignasego, Italy), following pupil dilatation with 1.0% tropicamide and 2.5% phenylephrine hydrochloride, and 5 minutes of visual dark adaptation, as described previously.[30–32] Light stimuli were presented randomly during the examination. Results are reported in decibels. Stability of fixation was expressed as the bivariate contour ellipse area (BCEA), which is the area of an ellipse on the retinal surface within which the center of the target was imaged 68% of the time. BCEA is a standardized measure that provides a means for quantification and comparison of fixation stability. Smaller BCEA values correspond to more precise fixation.[33]

Microperimetric Data Analysis

"En face" OCT images and microperimetric retinal sensitivity threshold data were superimposed over images of the fundus and adjusted as necessary to attain exact correspondence. To reduce bias from conditions unrelated to type 2 MacTel, only data from test points within the central 10° of the MP1 grid were considered in calculations. Sensitivity thresholds measured within retinal areas corresponding to a break in the IS/OS junction layer were compared to those measured external to the lesion. Further, to characterize the relationship of IS/OS break area and retinal function, the aggregate sensitivity loss was calculated. Background sensitivity was defined as the average of retinal sensitivity values measured at test points outside the area of the IS/OS break. To obtain the aggregate retinal sensitivity loss, the difference relative to the background sensitivity was calculated at each test point within the area of the IS/OS break and these differences were summed. Aggregate loss (expressed in decibels [dB]) thus correlates directly with lesion area and also reflects scotoma depth in a single variable.

Statistical Methods

Analyses were conducted using commercially available statistical software (IBM SPSS Statistics version 17; IBM Corporation, Armonk, NY and SAS version 9.02; SAS Institute, Cary, NC). A P value of < 0.05 was accepted as statistically significant.

Results

Patient Characteristics

We examined 49 eyes of 28 patients from one site in the MacTel Study with available SD-OCT volume scans. Patients ranged from 46 to 77 years in age (mean 62.6 years, SD 9.4 years), and 13 were males and 15 females. Approximately 27% of eyes had minor abnormal pigmentation, while the remaining eyes had less severe changes associated with type 2 MacTel.

Imaging

A total of 74 OCT volume scans was processed for this study. The Q factor (Topcon-specific quality factor reflecting signal strength) ranged from 25.0 to 75.3 (mean 56.9, SD 11.5). To assess the utility of "en face" imaging in real-life situations, no scan was excluded based on a low Q-factor alone. Motion artifacts due to microsaccades and/or drifts larger than 100 μm were present in 14 volume scans. In 4 cases, these were outside the region of interest (ROI) and were ignored. Eye movements were parallel to B-scan direction within the ROI in 10 cases and misalignments between B-scans could be corrected. In 6 cases the eye movements had a major component perpendicular to the B-scan. In 2 cases this resulted in a resampling of the same retinal area two or more times; in one case this could be corrected. In 4 cases vertical saccades resulted in scans of disparate retinal areas, and these scans were not used. One volume scan intended for assessment of variability was discarded due to axial eye/head movements

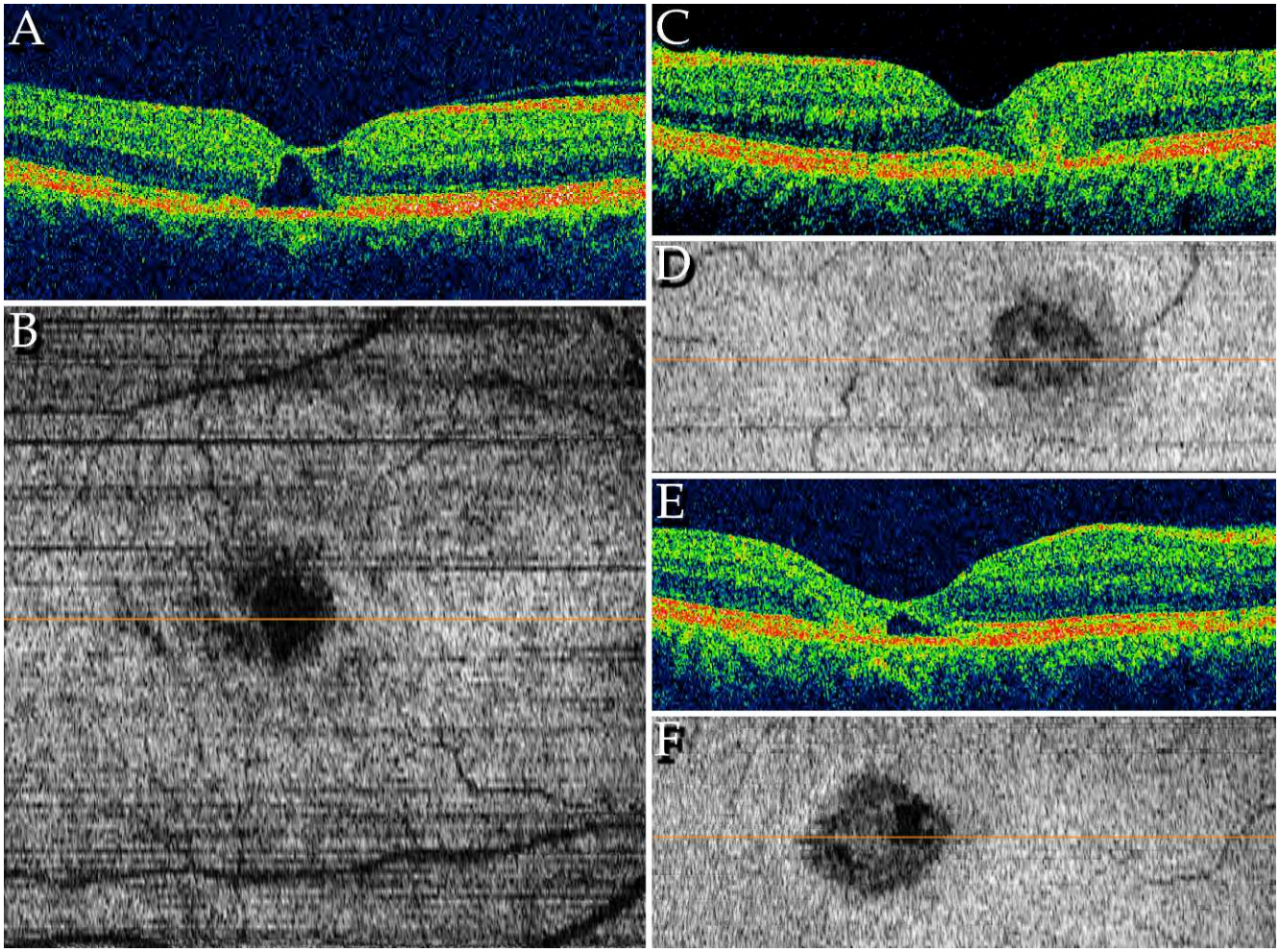

Figure 1. The IS/OS lesion in OCT "en face" and corresponding B-scan images. (**A**) Representative B-scan of a type 2 MacTel eye, from a 6×6 mm volume consisting of 128 B-scans. (**B**) The en face image of the full scan area on the level of the IS/OS line, showing the shadowgram of the retinal blood vessels. The dark area toward the center of the image corresponds to the outer retinal "empty space" seen in (**A**), the dark grey area around it is the IS/OS break. Horizontal dark stripes are due to minor axial misalignments between the individual B-scans. (**C**, **D**, **E**, **F**) Illustrate the pathologic "collapsing layers" extending between the inner and outer retina. Orange horizontal lines mark the position of respective B-scan within the corresponding en face image.

during the scan. Uneven field illumination was noted in 5 scans.

The IS/OS break appears as a darker area within the en face image against the background of the highly reflective IS/OS layer (Fig. 1). The edges of the break varied from sharp to indistinct, corresponding to a sudden discontinuity or gradual loss of reflectivity respectively. Near-black (low-reflective) areas were apparent internal to the edges of the lesion in some cases. These corresponded to cross-sections of outer retinal empty spaces at the level of the IS/OS junctions. Structures with a reflectivity similar to that of the IS/OS also were apparent within some lesions. In some cases these corresponded to islands of preserved IS/OS, but more frequently to the cross section of an area with pathologic vertical restructuring of the retina. Retinal layers between the outer plexiform layer and the RPE in these areas seemed to be absent, while the disorganized outer plexiform layer and layers interior to it gave the impression of "collapsing" onto the RPE (Figs. 1C–E).

Total IS/OS break areas ranged from 0.039 to 2.229 mm^2 (mean 0.627 mm^2, SD 0.529 mm^2) in right eyes and from 0.027 to 1.494 mm^2 (mean 0.492 mm^2, SD 0.422 mm^2) in left eyes. A strong positive correlation between lesion area in left and right eyes was found (Spearman correlation $\rho = 0.770$, $P < 0.01$, $n = 42$, Fig. 2A). When repeatability of IS/OS lesion area measurements was assessed by processing two consecutive scans of 19 eyes the intra-class correlation coefficient was 0.99 (95% confidence interval [CI] of 0.975–0.996).

Topographically, the IS/OS lesion was located typically on the temporal side of the fovea, in 65% reaching the center of the foveal depression. Mean radial distance of the nearest lesion edge from the foveal center was 158 μm (SD 220 μm, range 10–890 μm) in cases sparing the foveal center, and 126 μm (SD 125 μm, range 15–560 μm) in cases involving the foveal center. A positive correlation was found between break area and degree of involvement of the foveal center in right eyes (Spearman correlation $\rho = 0.44$, $P < 0.05$, $n = 25$) as well as in left eyes ($\rho = 0.58$, $P < 0.01$, $n = 24$).

An oval ring or ring segments with a backscatter lower than that of the IS/OS was apparent around the IS/OS break in 25 eyes (51%, Figs. 2B, 2C). In 4 cases this ring was accompanied by one of higher reflectivity than the surrounding IS/OS layer (Fig. 4).

Retinal Function

BCVA. BCVA ranged from 46 to 89 letters (mean 72.4 letters, Snellen equivalent of 20/40, SD 9.7 letters) in right

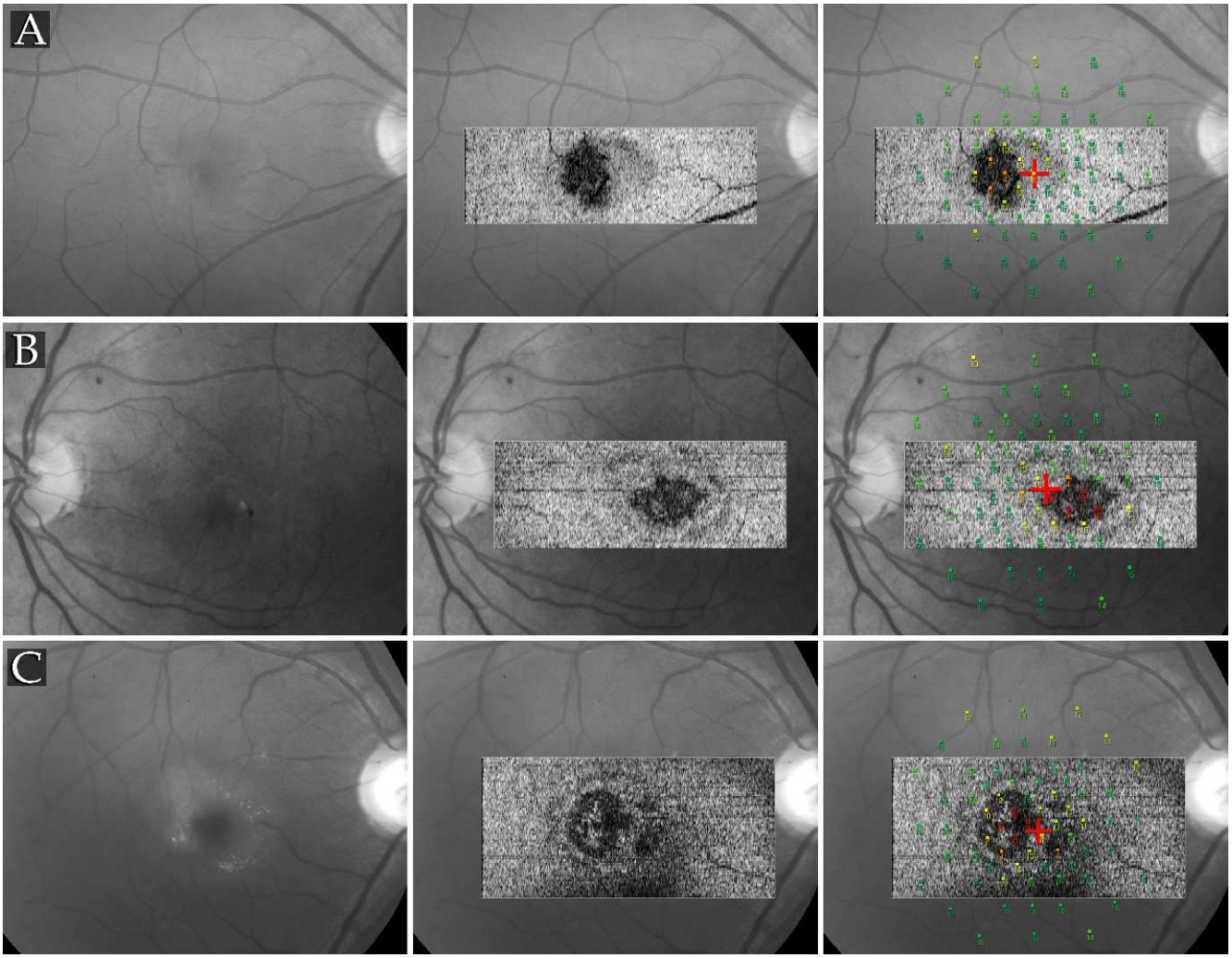

Figure 2. Functional correlates of the IS/OS break. *Left column*: RF fundus image. *Middle column*: RF with the "en face" OCT image superimposed. *Right column*: MP1 mesopic retinal sensitivity maps superimposed. Significantly higher thresholds were measured over areas with an IS/OS break, the highest loss co-localizing with the "collapsing layers." (**B**, **C**) Segments of a ring with lower reflectance encircling the central IS/OS break area apparent. In many cases a corresponding pattern is discernible in infrared images of the fundus.

eyes, and from 41 to 85 letters (mean 71.4 letters, Snellen equivalent of 20/40, SD 10.8 letters) in left eyes. Eyes in which the foveal center was affected by the lesion had a mean letter score of 71.1 (range 41–89, SD 11.2), eyes with no detectable lesion at the foveal center had a mean letter score of 73.3 (range 58–84, SD 7.9), differences were not statistically significant ($P = 0.47$, Student's *t*-test)

Microperimetry. Retinal areas corresponding to a break in the IS/OS layer showed a mean retinal sensitivity of 8.3 dB (median 10.0 dB, SD 5.8 dB) in right eyes and 8.7 dB (median 10.0 dB, SD 5.7 dB) in left eyes. Mean sensitivity over retinal areas not within the lesion was 17.0 dB (median 18.0 dB, SD 3.3 dB) in right eyes and 16.7 dB (median 18.0 dB, SD 3.6 dB) in left eyes. Differences in retinal sensitivity loss between affected and unaffected areas were statistically significant (paired *t* test, $P < 0.01$ in right and left eyes). Mean aggregate retinal sensitivity loss was 33.5 dB (median 27.9 dB, SD 30.4, $n = 40$), a positive correlation with IS/OS lesion area was present (Pearson correlation coefficient = 0.848, $P < 0.01$, Fig. 2B, data were normally distributed). The topographic distribution of retinal sensitivity loss corresponded closely to that of the IS/OS break area (Fig. 3).

Fixation Stability. BCEA ranged from $0.46^{\circ 2}$ to $16.99^{\circ 2}$ (mean $4.69^{\circ 2}$, SD $4.10^{\circ 2}$) in right eyes, and from $0.47^{\circ 2}$ to $13.34^{\circ 2}$ (mean $4.71^{\circ 2}$, SD $3.73^{\circ 2}$) in left eyes. A statistically significant correlation with IS/OS lesion area or radial distance of the nearest edge of the lesion from the foveal center was not detectable.

Discussion

In our study, we isolated backscatter information from the level of the line attributed to the photoreceptor IS/OS junctions to develop a more sensitive structural predictor of vision loss in type 2 MacTel. By 3D processing of standard volume scan data from a commercially available SD-OCT device and imaging the data "en face," we demonstrated the characteristics of a break in this layer. This break was closely associated with a loss of mesopic retinal sensitivity. These findings are significant not just to allow more sensitive monitoring of the condition, but also as an outcome in trials of potential treatments.

"En face" OCT imaging of the retina is intuitive for the examiner, and permits 2D assessment of lesion extent, topographical analysis, and close comparisons with other

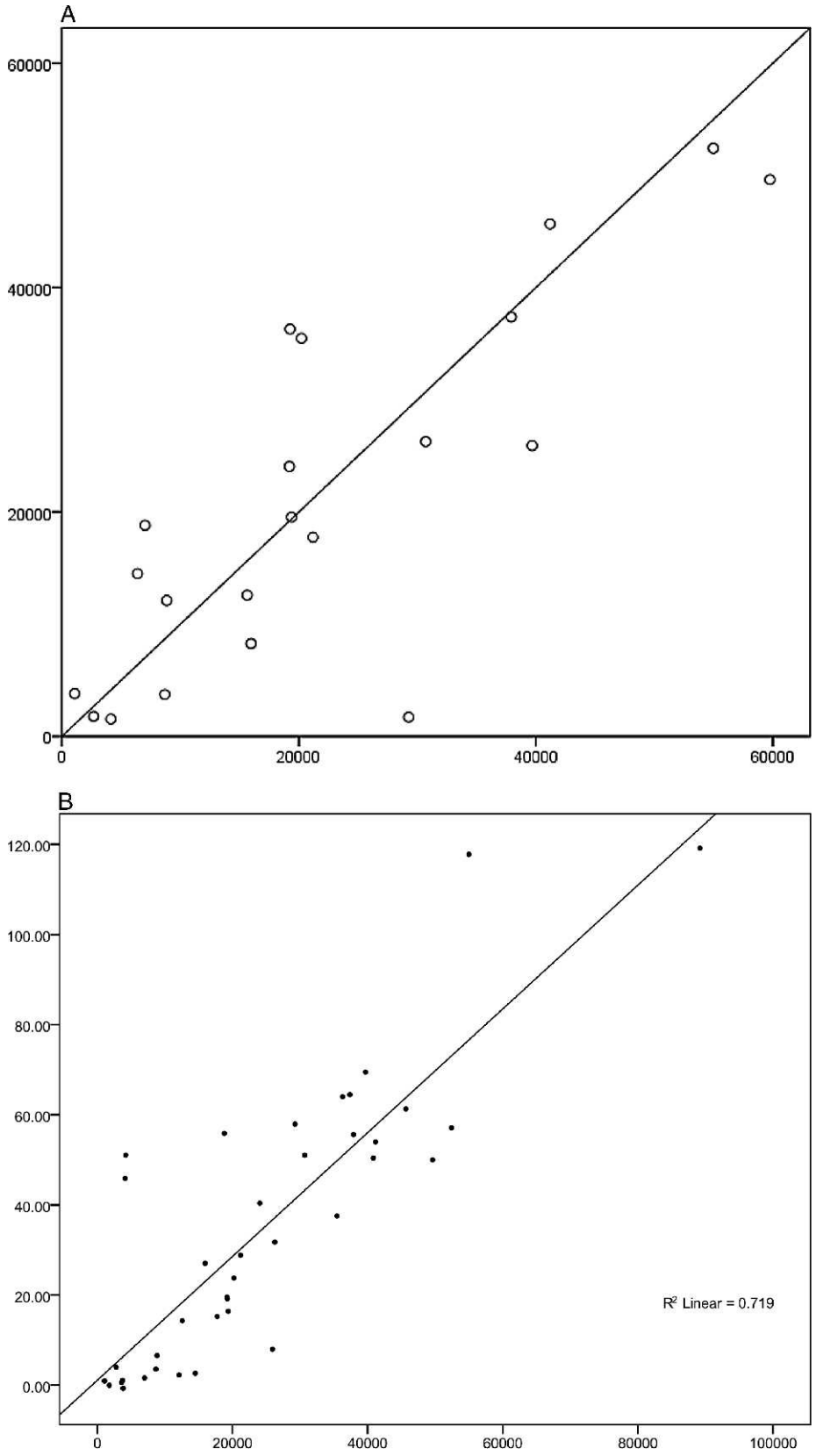

Figure 3. (**A**) IS/OS break area (pixels) in fellow eyes (x-axis, left eyes; y-axis right eyes; Spearman correlation $\rho = 0.770$, $P < 0.01$). (**B**) Correlation between IS/OS break area in pixels (x-axis) and aggregate retinal sensitivity loss (dB). Pearson correlation coefficient = 0.848, $P < 0.01$.

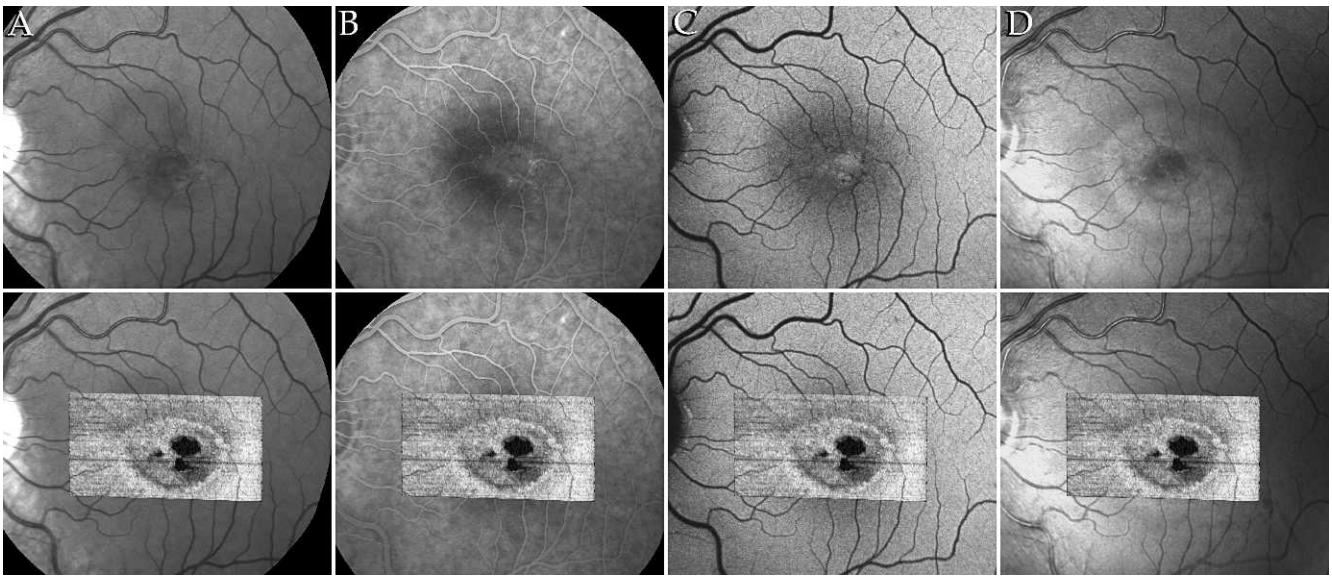

FIGURE 4. In some "en face" images, a highly reflective ring around the central lesion was seen. A similar pattern was not apparent outside the IS/OS layer within the OCT volume or in other imaging modalities (columns [**B**] FFA and [**C**] FAF), except in the confocal blue light reflectance image (**D**) and partially in the infrared (**A**).

imaging modalities. Prototype OCT systems using a C-mode configuration, performing single planar, 2D transverse scans[34,35] (i.e., "en face," in the coronal plane) as well as 3D volume scans[36] have been developed. It also has been demonstrated in experimental OCT systems producing 3D volumes of traditional axial scans that OCT "en face" fundus images can be created by summing reflectivity data in A scans,[37] and that backscatter intensity information specific to selected slabs or individual retinal layers also can be extracted.[19,38]

In our study we used volume scans from a standard, commercially available SD-OCT machine that was not equipped with a real-time eye-tracking system. Since fixation stability in type 2 MacTel patients typically is affected early, motion artifacts may be a major source of error. We acknowledge that in the absence of vascular landmarks, in some "en face" images, near the foveal center, it may not be possible to detect artifacts due to minor eye movements. However, in 19 of 20 double scans performed consecutively in our study, lesion area measurements showed a high degree of reproducibility between scans and over time. In one case, one scan of a pair had to be discarded due to obvious inappropriate axial movement by the patient. Performing two consecutive scans routinely may reduce the risk of undetected motion artifacts further. Machines with active eye-tracking do, however, have a significant advantage.

We performed manual segmentation of the IS/OS line. Several methods for automated segmentation of retinal layers have been published previously.[27,39–42] However, extensive discontinuities in and reduced backscatter from the IS/OS are common near the foveal center in type 2 MacTel, which may cause errors in automated boundary detection. Manual segmentation was deemed to provide more accurate results.

Type 2 MacTel is associated with evidence of retinal neurodegeneration that is integral to the disorder. Imaged "en face" at the level of the IS/OS line, the most prominent feature of eyes with type 2 MacTel is the break in the IS/OS line, which appears dark against the highly reflective background of the IS/OS. Its boundaries may be distinct but also indistinct. Where the edge is indistinct, the IS/OS line often appears in B-scans thinner and deviates toward the choroid from its expected location, which may correspond to a shortening of the photoreceptor outer segments and a disorganization of the IS/OS junctions. An attenuated signal from the IS/OS also may in itself be a sign of photoreceptor damage.[43] It is possible that the "IS/OS line" may not be representative of the IS/OS junctions. Recent studies indicate that this line may, in fact, align with the ellipsoids of the photoreceptor inner segments.[43–45] Its functional relevance, however, is well established.

Within the area of the break, regions with very low backscatter may be present. These correspond to the cross sections of outer retinal spaces with low reflectivity. In B-scans, these spaces give the impression of degenerative cavities, typically without signs of internal pressure. The material within these spaces does not take up fluorescein even in the late phase of fluorescein angiography.

Insular areas with a reflectivity closer to that of the IS/OS also were apparent within breaks. These may correspond to areas with preserved IS/OS, but also to the cross sections of an abnormal retinal tissue with a vertical reorganization, where retinal layers between the outer plexiform layer and the RPE seem to be absent and the structurally disorganized remaining layers give the impression of "collapsing" onto the RPE. In cases where the break did not reach the foveal center, this structure always was seen on its temporal side. Based on "en face" images alone it may not be possible in all cases to determine whether a lighter area within the break represents an island of preserved IS/OS or "collapsed" layers, necessitating a review of the corresponding B-scans.

In approximately half of the eyes examined, a dark ring or arc fragments of a ring around the central break were apparent in the "en face" image. In a few cases an additional bright ring was visible. This phenomenon appeared restricted to the IS/OS layer, a corresponding pattern could not be demonstrated in other layers of the retina, and it does not seem to be related to the artifactual ring emanating from specular reflection mainly from the surface of the retina.[46] The origin and significance of this ring are unclear; however, it's similarity in location and shape to the area in which Powner et al. found Müller cell loss or dysfunction within the central macula is remarkable.[47]

We found a statistically significant elevation in mesopic sensitivity thresholds within the area of the IS/OS lesion. The difference between mean sensitivities within the break area and the background was just over 8 dB, which is similar to the

sensitivity loss reported by other investigators associated with an IS/OS break, despite the differences in underlying disease and methods used.[8,48]

Chen et al. found (in 50 predominantly AMD eyes) the coefficients of repeatability for MP1 central macular sensitivity (CMS, inside 10°) to be 2.56 dB, of paracentral macular sensitivity (PMS, 10–20° ring) 2.13 dB and point-wise sensitivity (PWS) 5.56 dB.[49] They recommended the use of CMS and PMS for monitoring macular function, and considered a change of greater than 2.56 and 2.31 dB significant, respectively. Relative to these levels, the differences in our study are significant not just statistically, but also with respect to repeatability. We also found a statistically highly significant positive correlation between IS/OS break area and aggregate sensitivity loss. While the low number of sensitivity test points did not allow a detailed analysis, it was noted that the highest sensitivity loss seemed to be associated with areas of "collapsed layers."

Traditional imaging modalities (color fundus photography and fluorescein angiography) have limitations. In these, the most prominent features of type 2 MacTel are vascular.[50] Loss of retinal transparency is highly dependent on image quality, and abnormal pigment may accompany otherwise few or mild signs of the disease and also may be absent altogether before neovascularization. These signs also may be challenging to quantify especially in early disease.

New techniques, like SD-OCT (and dual wavelength autofluorescence or blue light reflectance) imaging, have introduced new means for assessing neurodegenerative change in type 2 MacTel. The IS/OS lesion in "en face" SD-OCT images is readily quantifiable and closely associated with function loss such that it may be a prime candidate for a structural outcome measure for following disease progression in the natural history as well as in interventional studies of type 2 MacTel. Further investigations are necessary to determine the progression characteristics of the IS/OS break over time.

Acknowledgments

Austin Roorda, PhD, provided valuable discussions concerning the optical properties of the retina. Marcus Fruttiger, PhD, provided valuable discussions concerning microanatomic, histologic, and cell biologic aspects of type 2 MacTel.

References

1. Gass JD, Oyakawa RT. Idiopathic juxtafoveolar retinal telangiectasis. *Arch Ophthalmol*. 1982;100:769–780.
2. Gaudric A, Ducos de Lahitte G, Cohen SY, Massin P, Haouchine B. Optical coherence tomography in group 2A idiopathic juxtafoveolar retinal telangiectasis. *Arch Ophthalmol*. 2006; 124:1410–1419.
3. Yannuzzi LA, Bardal AM, Freund KB, Chen KJ, Eandi CM, Blodi B. Idiopathic macular telangiectasia. *Arch Ophthalmol*. 2006; 124:450–460.
4. Maruko I, Iida T, Sekiryu T, Fujiwara T. Early morphological changes and functional abnormalities in group 2A idiopathic juxtafoveolar retinal telangiectasis using spectral domain optical coherence tomography and microperimetry. *Br J Ophthalmol*. 2008;92:1488–1491.
5. Krivosic V, Tadayoni R, Massin P, Erginay A, Gaudric A. Spectral domain optical coherence tomography in type 2 idiopathic perifoveal telangiectasia. *Ophthalmic Surg Lasers Imaging*. 2009;40:379–384.
6. Ota M, Tsujikawa A, Murakami T, et al. Foveal photoreceptor layer in eyes with persistent cystoid macular edema associated with branch retinal vein occlusion. *Am J Ophthalmol*. 2008; 145:273–280.
7. Maheshwary AS, Oster SF, Yuson RM, Cheng L, Mojana F, Freeman WR. The association between percent disruption of the photoreceptor inner segment-outer segment junction and visual acuity in diabetic macular edema. *Am J Ophthalmol*. 2010;150:63.e61–67.e61.
8. Rangaswamy NV, Patel HM, Locke KG, Hood DC, Birch DG. A comparison of visual field sensitivity to photoreceptor thickness in retinitis pigmentosa. *Invest Ophthalmol Vis Sci*. 2010;51:4213–4219.
9. Park SJ, Woo SJ, Park KH, Hwang JM, Chung H. Morphologic photoreceptor abnormality in occult macular dystrophy on spectral-domain optical coherence tomography. *Invest Ophthalmol Vis Sci*. 2010;51:3673–3679.
10. Landa G, Su E, Garcia PM, Seiple WH, Rosen RB. Inner segment-outer segment junctional layer integrity and corresponding retinal sensitivity in dry and wet forms of age-related macular degeneration. *Retina*. 2011;31:364–370.
11. Eandi CM, Chung JE, Cardillo-Piccolino F, Spaide RF. Optical coherence tomography in unilateral resolved central serous chorioretinopathy. *Retina*. 2005;25:417–421.
12. Yamauchi Y, Agawa T, Tsukahara R, et al. Correlation between high-resolution optical coherence tomography (OCT) images and histopathology in an iodoacetic acid-induced model of retinal degeneration in rabbits. *Br J Ophthalmol*. 2011;95: 1157–1160.
13. Chang LK, Koizumi H, Spaide RF. Disruption of the photoreceptor inner segment-outer segment junction in eyes with macular holes. *Retina*. 2008;28:969–975.
14. Spaide RF, Koizumi H, Freund KB. Photoreceptor outer segment abnormalities as a cause of blind spot enlargement in acute zonal occult outer retinopathy-complex diseases. *Am J Ophthalmol*. 2008;146:111–120.
15. Wang NK, Chou CL, Lima LH, et al. Fundus autofluorescence in cone dystrophy. *Doc Ophthalmol*. 2009;119:141–144.
16. Hood DC, Lazow MA, Locke KG, Greenstein VC, Birch DG. The transition zone between healthy and diseased retina in patients with retinitis pigmentosa. *Invest Ophthalmol Vis Sci*. 52:101–108.
17. Paunescu LA, Ko TH, Duker JS, et al. Idiopathic juxtafoveal retinal telangiectasis: new findings by ultrahigh-resolution optical coherence tomography. *Ophthalmology*. 2006;113:48–57.
18. Charbel Issa P, Troeger E, Finger R, Holz FG, Wilke R, Scholl HP. Structure-function correlation of the human central retina. *PLoS ONE*. 2010;5:e12864.
19. Wojtkowski M, Srinivasan V, Fujimoto JG, et al. Three-dimensional retinal imaging with high-speed ultrahigh-resolution optical coherence tomography. *Ophthalmology*. 2005; 112:1734–1746.
20. Rosen RB, Hathaway M, Rogers J, et al. Multidimensional en-face OCT imaging of the retina. *Opt Express*. 2009;17:4112–4133.
21. Jiao S, Wu C, Knighton RW, Gregori G, Puliafito CA. Registration of high-density cross sectional images to the fundus image in spectral-domain ophthalmic optical coherence tomography. *Opt Express*. 2006;14:3368–3376.
22. Guo L, Tsatourian V, Luong V, et al. En face optical coherence tomography: a new method to analyse structural changes of the optic nerve head in rat glaucoma. *Br J Ophthalmol*. 2005; 89:1210–1216.
23. Rogers J, Podoleanu A, Dobre G, Jackson D, Fitzke F. Topography and volume measurements of the optic nerve using en-face optical coherence tomography. *Opt Express*. 2001;9:533–545.
24. Gorczynska I, Srinivasan VJ, Vuong LN, et al. Projection OCT fundus imaging for visualising outer retinal pathology in non-exudative age-related macular degeneration. *Br J Ophthalmol*. 2009;93:603–609.

25. Wojtkowski M, Sikorski BL, Gorczynska I, et al. Comparison of reflectivity maps and outer retinal topography in retinal disease by 3-D Fourier domain optical coherence tomography. *Opt Express*. 2009;17:4189–4207.
26. Oh J, Smiddy WE, Flynn HW Jr, Gregori G, Lujan B. Photoreceptor inner/outer segment defect imaging by spectral domain OCT and visual prognosis after macular hole surgery. *Invest Ophthalmol Vis Sci*. 2010;51:1651–1658.
27. Wanek J, Zelkha R, Lim JI, Shahidi M. Feasibility of a method for en face imaging of photoreceptor cell integrity. *Am J Ophthalmol*. 2011;152:807.e1–814.e1.
28. Early Treatment Diabetic Retinopathy Study design and baseline patient characteristics. ETDRS report number 7. *Ophthalmology*. 1991;98(suppl 5):741–756.
29. Ferris FL III, Kassoff A, Bresnick GH, Bailey I. New visual acuity charts for clinical research. *Am J Ophthalmol*. 1982;94: 91–96.
30. Rohrschneider K, Springer C, Bültmann S, Völcker HE. Microperimetry–comparison between the micro perimeter 1 and scanning laser ophthalmoscope–fundus perimetry. *Am J Ophthalmol*. 2005;139:125–134.
31. Midena E, Vujosevic S, Convento E, Manfre' A, Cavarzeran F, Pilotto E. Microperimetry and fundus autofluorescence in patients with early age-related macular degeneration. *Br J Ophthalmol*. 2007;91:1499–1503.
32. Schmitz-Valckenberg S, Ong EE, Rubin GS, et al. Structural and functional changes over time in MacTel patients. *Retina*. 2009; 29:1314–1320.
33. Crossland MD, Dunbar HM, Rubin GS. Fixation stability measurement using the MP1 microperimeter. *Retina*. 2009; 29:651–656.
34. Podoleanu AG, Dobre GM, Jackson DA. En-face coherence imaging using galvanometer scanner modulation. *Opt Lett*. 1998;23:147–149.
35. Cucu RG, Podoleanu AG, Rogers JA, Pedro J, Rosen RB. Combined confocal/en face T-scan-based ultrahigh-resolution optical coherence tomography in vivo retinal imaging. *Opt Lett*. 2006;31:1684–1686.
36. Hitzenberger C, Trost P, Lo PW, Zhou Q. Three-dimensional imaging of the human retina by high-speed optical coherence tomography. *Opt Express*. 2003;11:2753–2761.
37. Jiao S, Knighton R, Huang X, Gregori G, Puliafito C. Simultaneous acquisition of sectional and fundus ophthalmic images with spectral-domain optical coherence tomography. *Opt Express*. 2005;13:444–452.
38. Kaluzny JJ, Wojtkowski M, Sikorski BL, et al. Analysis of the outer retina reconstructed by high-resolution, three-dimensional spectral domain optical coherence tomography. *Ophthalmic Surg Lasers Imaging*. 2009;40:102–108.
39. Hee MR, Puliafito CA, Duker JS, et al. Topography of diabetic macular edema with optical coherence tomography. *Ophthalmology*. 1998;105:360–370.
40. Koozekanani D, Boyer K, Roberts C. Retinal thickness measurements from optical coherence tomography using a Markov boundary model. *IEEE Trans Med Imaging*. 2001;20: 900–916.
41. Szkulmowski M, Wojtkowski M, Sikorski B, et al. Analysis of posterior retinal layers in spectral optical coherence tomography images of the normal retina and retinal pathologies. *J Biomed Opt*. 2007;12:041207.
42. Srinivasan VJ, Monson BK, Wojtkowski M, et al. Characterization of outer retinal morphology with high-speed, ultrahigh-resolution optical coherence tomography. *Invest Ophthalmol Vis Sci*. 2008;49:1571–1579.
43. Hood DC, Zhang X, Ramachandran R, et al. The inner segment/outer segment border seen on optical coherence tomography is less intense in patients with diminished cone function. *Invest Ophthalmol Vis Sci*. 52:9703–9709.
44. Spaide RF, Curcio CA. Anatomical correlates to the bands seen in the outer retina by optical coherence tomography: literature review and model. *Retina*. 31:1609–1619.
45. Fernandez EJ, Hermann B, Povazay B, et al. Ultrahigh resolution optical coherence tomography and pancorrection for cellular imaging of the living human retina. *Opt Express*. 2008;16:11083–11094.
46. Sikorski BL, Wojtkowski M, Kaluzny JJ, Szkulmowski M, Kowalczyk A. Correlation of spectral optical coherence tomography with fluorescein and indocyanine green angiography in multiple evanescent white dot syndrome. *Br J Ophthalmol*. 2008;92:1552–1557.
47. Powner MB, Gillies MC, Tretiach M, et al. Perifoveal Müller cell depletion in a case of macular telangiectasia type 2. *Ophthalmology*. 2010;117:2407–2416.
48. Hood DC, Ramachandran R, Holopigian K, Lazow M, Birch DG, Greenstein VC. Method for deriving visual field boundaries from OCT scans of patients with retinitis pigmentosa. *Biomed Opt Express*. 2011;2:1106–1114.
49. Chen FK, Patel PJ, Xing W, et al. Test-retest variability of microperimetry using the Nidek MP1 in patients with macular disease. *Invest Ophthalmol Vis Sci*. 2009;50:3464–3472.
50. Gass JD, Blodi BA. Idiopathic juxtafoveolar retinal telangiectasis. Update of classification and follow-up study. *Ophthalmology*. 1993;100:1536–1546.

Appendix

Participating Principal Investigators and Centers in the MacTel Study

Jose-Alain Sahel, Centre Hopitalier National D'Optalmologie des Quinze-Vingts, Paris, France.
Robyn Guymer, Centre for Eye Research, East Melbourne, Australia.
Gisele Soubrane, Clinique Ophtalmolgie de Creteil, Creteil, France.
Alain Gaudric, Hopital Lariboisiere, Paris, France.
Steven Schwartz, Jules Stein Eye Institute, UCLA, Los Angeles, CA.
Ian Constable, Lions Eye Institute, Nedlands, Australia.
Michael Co-oney, Manhattan Eye, Ear, & Throat Hospital, New York, NY.
Catherine Egan, Moorfields Eye Hospital, London, England.
Lawrence Singerman, Retina Associates of Cleveland, Cleveland, OH.
Mark C. Gillies, Save Sight Institute, Sydney, Australia.
Martin Friedlander, Scripps Research Institute, La Jolla, CA.
Daniel Pauleikhoff, St. Franziskus Hospital, Muenster, Germany.
Joseph Moisseiev, The Goldschleger Eye Institute, Tel Hashomer, Israel.
Richard Rosen, The New York Eye and Ear Infirmary, New York, NY.
Robert Murphy, The Retina Group of Washington, Fairfax, VA.
Frank Holz, University of Bonn, Bonn, Germany.
Grant Comer, University of Michigan, Kellogg Eye Center, Ann Arbor, MI.
Barbara Blodi, University of Wisconsin, Madison, WI.
Diana Do, The Wilmer Eye Institute, Baltimore, MD.
Alexander Brucker, Scheie Eye Institute, Philadelphia, PA.
Raja Narayanan, LV Prasad Eye Institute, Hyderabad, India.
Sebastian Wolf, University of Bern, Bern, Switzerland.
Philip Rosenfeld, Bascom Palmer, Miami, FL.
Paul S. Bernstein, Moran Eye Center, University of Utah, UT.
Joan W. Miller, Massachusetts Eye and Ear Infirmary, Harvard Medical School, Boston, MA.